Verification of precipitation type measurements in an inner valley

Author: Marta Balagué Martínez
Supervisor: Joan Bech Rustullet
Facultat de Física, Universitat de Barcelona, Diagonal 645, 08028 Barcelona, Spain.

Abstract: This study examines various methodologies for classifying precipitation types at both surface and upper levels in La Cerdanya valley through the implementation of a fuzzy verification framework. By comparing on-site observations from Micro Rain Radars (MRR2, MRR-Pro) with the operational product Rain or Snow (ROS), distinct performances are revealed. At the surface level, ROS displays a high Probability of Detection (POD) for precipitation but also a high False Alarm Ratio (FAR) when compared to MRR2. ROS detects some events that MRR2 misses, which contributes to the high FAR, and is likely due to its ability to identify light and scattered precipitation across the valley while MRRs are only able to detect it above their position. When compared to MRR-Pro, ROS exhibits a lower FAR but also a relatively low POD, suggesting that MRR-Pro captures finer transitional details that ROS is not able to. In terms of surface-type classification, both MRR2 and ROS identify rain and sporadic mixed and snow events evenly, while MRR-Pro observes a wider distribution of all types. Overall, ROS and MRR2 exhibit comparable performance in discriminating precipitation types at surface level within the valley, unlike MRR-Pro. In addition, ROS's estimates of height profiles using a digital elevation model show consistency with the observations from the MRRs, accurately indicating descending snow levels in several case studies.

I. INTRODUCTION

Classifying precipitation types in real-time is crucial for numerous hydrometeorological applications. It is particularly relevant for detecting transitions from rain to snow in mountainous regions and inner valleys.

Valleys often exhibit unique micro-climates and weather patterns compared to the surrounding higher elevations. They are prone to cold-air pools or temperature inversions, where cooler air is trapped near the surface level inside the valley. These conditions significantly influence the type of precipitation that occurs, resulting in various transitions between precipitation types. Therefore, understanding these dynamics is essential for precise weather diagnosis and forecasting.

The Meteorological Service of Catalonia (SMC) currently executes an operational product called Rain or Snow, for real-time monitoring of precipitation types across Catalonia (*Casellas et al.* 2021). This product utilizes an interpolated surface temperature and moisture field based on data collected from automatic weather stations. Precipitation types are determined by considering specific temperature thresholds, and the resulting field is then combined with data from the SMC radar network.

This study is part of a project involving a methodology called Single-Polarization Radar-based Simplified Hydrometeor Classification (PANDORA), which utilizes K-band vertically pointing Doppler observations from Micro Rain Radar (models MRR2 and MRR-Pro) (*Garcia-Benadi et al.* 2020) and categorizes precipitation type at surface and upper levels.

Data collection up to about 6 km above ground level (agl), took place at the Das Aerodrome in La Cerdanya (Eastern Spanish Pyrenees) over a five-month period. This region is known for its complex meteorological conditions, influenced by its east-north-east to west-south-west orientation.

The main objective of this work is to assess the effectiveness of the operational product against the PANDORA methodology in classifying precipitation types, utilizing a fuzzy verification approach (*Ebert* 2008). Fuzzy verification is relevant in this case because it provides more flexibility in matches between observations, thus offering a more comprehensive performance assessment in such a complex terrain region.

The study area and instruments considered are detailed in Section II. Section III describes the methodology, while Section IV presents the results for surface verification and height qualitative evaluation. Concluding remarks are provided in Section V. Additionally, an appendix is included with the equations used in the verification process and a standard definition of a 2x2 contingency table.

II. AREA OF STUDY AND INSTRUMENTS

A. La Cerdanya Valley

La Cerdanya (Figure 1) is an area situated in the eastern Pyrenees within the Segre River drainage basin. It is distinctive from other Pyrenean valleys due to its orientation, which is east-north-east to west-south-west rather than the more prevalent north-south direction. The lowest portion of the valley, which is roughly 15 kilometers wide and flat-bottomed, has an average elevation of about 1000 meters above sea level (asl). To the north and south, mountain ranges above 2000 meters asl enclose the valley. To the east, the terrain ascends to the Col de la Perche (1500 m asl) before descending into Conflent, which drains northeastward to the Mediterranean. To the west, the Segre River flows through a narrow gorge, restricting the down-valley flow.

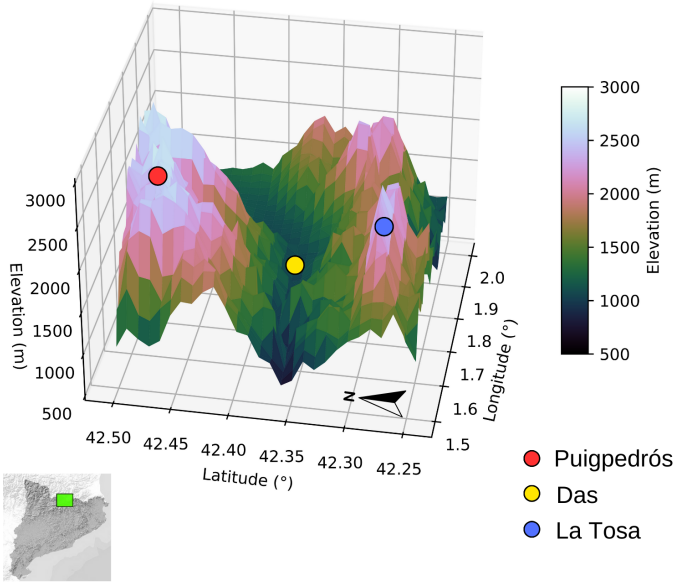

Figure 1. 3D map of La Cerdanya, displaying high mountains for reference on both sides: Puigpedrós (red circle) and La Tosa (blue circle), as well as the observing location on Das Aerodrome (yellow circle). The location of the region, on the eastern side of the Pyrenees mountain massif in Catalonia (green square) and the north direction are also indicated.

Because of the topography's shielding effect, La Cerdanya is especially vulnerable to temperature inversions during the winter (*Conangla et al.* 2018). While the surrounding higher altitude regions receive around 1000 mm year^{-1}, the inner valley experiences semi-arid, nearly continental conditions with an average of 500 mm of annual precipitation, indicating a rain shadow pattern (*SMC* 2024). In contrast to other Mediterranean locations, summer in Cerdanya is characterized by frequent convective showers, making it the wet season. However, due to challenges in accurately measuring solid precipitation with rain gauges (*Kochendorfer et al.* 2017), winter precipitation may be underestimated in climatology.

Snowfall distribution varies with altitude; the inner valley records fewer than 20 snow days per year, while the higher surrounding areas, especially those exposed to winter northerly winds, can experience more than 40 snow days per year (*Xercavins* 1985).

According to *González et al.* (2021), there can be a decoupling between the free atmosphere air above the mountain crest level and the stalled air of the valley, as evidenced by an increase in turbulence. Wind shear layer development has also been shown to enhance riming and aggregation of ice and snow particles.

Therefore, this area is particularly interesting for a vast number of reasons: the effect of possible differences in features between leeward and windward precipitation, as well as the implications on estimates of precipitation due to partial radar beam blockage (*Bech et al.* 2003), which in this area is estimated between 30-50% with a minimum beam height of 2400 m asl for the closest radar, which is located in Puig d'Arques, Baix Empordà.

B. Micro Rain Radar

A Micro Rain Radar (MRR) is a vertical Doppler radar profiler manufactured by MeteK in Germany, operating in K-band at 24 GHz and using a frequency modulated continuous wave (FMWC). This device uses measured spectral power back-scatter intensity to produce profiles of precipitation characteristics and hydrometeor particle size distributions. The MRR signal is transmitted vertically into the atmosphere and scattered back to the antenna upon hitting raindrops or other hydrometeors. Falling particles cause a frequency shift between the emitted and received signals, which correlates with their falling velocity. Since drops of varying sizes fall at different velocities, the back-scattered signal contains a range of Doppler frequencies and, with these frequencies, radar integral parameters can be obtained.

From November 2023 to March 2024, two MRRs were installed at Das Aerodrome (1097 m asl), one being a MRR2 version and the other a MRR-Pro. MRR-Pro model was configured with a range gate resolution of 50 m and can extend up to 6400 m agl, whereas MRR-2 model range gate resolution was set to 100 m and a maximum vertical extension of 3100 m agl. Both devices have distinct temporal resolutions: MRR2 records data every 60 seconds, whereas MRR-Pro records data every 10 seconds. To ensure temporal consistency, MRR-Pro data was resampled (by selecting the most frequent category in the interval) to have a temporal resolution of 60 seconds.

In order to simplify this work, only 3 categories have been considered: rain, snow and mixed precipitation. The precipitation type for each minute of observation is obtained using the methodology developed by *Garcia-Benadi et al.* (2020), which consists of open code software that processes the spectral raw data to provide radar integral parameters and converts them into a hydrometeor classification.

A total of 168720 non-filtered minutes for MRR2 and 166621 minutes for MRR-Pro were recorded during the study period, and a quality control to filter noise was also applied with the following criteria.

A precipitation data point is considered valid if:

- At least 6 minutes of continuous precipitation is detected inside a rolling window containing the data point.
- There are at least 5 height bins with data.

If the previous two conditions are not met, that data point is set to 'No precipitation'. The total number of observations sorted for each class and instrument can be found in Table I.

Table I. Number of one-minute observations for MRR2 and MRR-Pro before and after applying the quality control.

	MRR2 (min)		MRR-Pro (min)	
Class	**Raw**	**Filtered**	**Raw**	**Filtered**
No data	4080	4080	6179	6179
Rain	11810	3639	6220	5157
Mixed	8943	224	2456	1840
Snow	4080	640	6179	4117
No precipitation	143887	164217	151766	155507

C. Rain or Snow Operational Product

The Rain or Snow (ROS) operational product developed by the SMC offers a nearly real-time spatial classification estimation of surface precipitation types. This product integrates data from the Automatic Weather Stations Network (XEMA) and WRF model outputs to calculate the wet bulb temperature field.

ROS uses three distinct colors to represent different precipitation types: red for rain, green for sleet (rain and snow mixed), and blue for snow. The differentiation between these types is based on specific wet bulb temperature thresholds as defined by *Casellas et al.* (2021):

- If the wet bulb temperature is greater than 1.1 °C, the precipitation at the surface is considered rain.
- If the wet bulb temperature is less than or equal to 0.7 °C, the precipitation at the surface is considered snow.
- If the wet bulb temperature falls between the two mentioned thresholds, the precipitation at the surface is considered sleet.

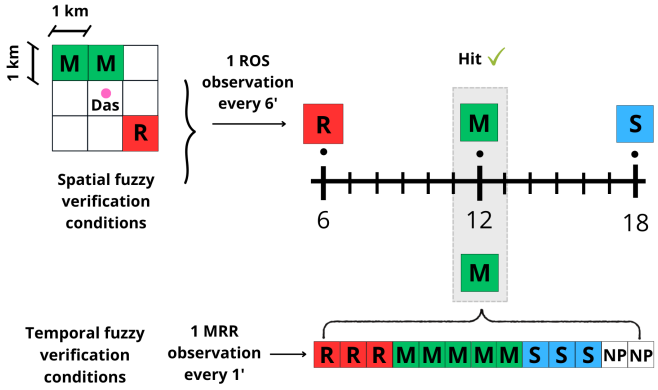

Figure 2. Example of the fuzzy verification framework comparing ROS and MRR observations of rain (R), mixed precipitation (M) and snow (S).

To generate the ROS product, the wet bulb temperature field is first obtained and classified according to the thresholds mentioned above. The radar reflectivity field from the SMC's Radar Network (XRAD) is also used to delineate areas of precipitation, and the final product is obtained by combining both fields. It is important to note that each network operates at different temporal resolutions: the automatic stations update every 30 minutes, whereas radars give new data every 6 minutes. This discrepancy means that temperature changes may be detected and integrated into the product with some delay.

Throughout the study, a total of 28663 ROS minutes were considered, aligning with the observation period of the MRRs. For consistency, sleet was categorized as mixed precipitation, acknowledging potential minor distinctions.

III. METHODOLOGY

A. Fuzzy Verification Framework

The verification of different hydrometeorological categories is challenging due to the inherent spatial and temporal variability of these phenomena. For example, transitions between mixed and snow precipitation can cause inaccuracies if the verification is restricted only to single data points.

In this work, an approach known as *'Fuzzy Verification'* has been implemented. First presented by *Ebert* (2008), the main idea is to relax the requirements for exact matches by considering a window or neighborhood in space and time rather than only focusing on isolated matching points. Fuzzy verification is typically used to assess forecast performance. However, in this study, it will be applied to compare two observational methods at surface level. Additionally, MRRs will be treated as the observation, and ROS as the forecast, despite ROS being a diagnostic tool.

For both MRRs, the surface data is inferred by selecting only the first range gate, 100 m agl for MMR2 and 50 m agl for MRR-Pro. Since ROS data has a temporal resolution of 6 minutes, while MRR2 and MRR-Pro provide data every minute, a ± 6 minute window will be used as a fuzzy temporal condition. For the spatial fuzzy condition, a 3x3 km grid, centered on ROS's surface-level pixel closest to the observation point, will be used. Figure 2 provides an example of the methodology applied for surface verification.

Two distinct issues need to be addressed: verifying the detection of precipitation (of any type) and verifying the type of precipitation. It is crucial to first define the events, specifically, we need to determine what constitutes a positive precipitation event for each detection methodology, following the example of *Garcia-Benadi et al.* (2022):

- MRR Precipitation: At least 1 min with precipitation in the ± 6 min window.

- MRR No Precipitation: No precipitation detected inside the window.
- ROS Precipitation: Every 6 min, at least 1 cell of the 3x3 km grid detected precipitation.
- ROS No Precipitation: No precipitation detected inside the grid.

Similarly, we need to establish what constitutes a positive event for each precipitation type:

- MRR Rain / Mixed / Snow: For every ± 6 minute window, the most frequently occurring type of precipitation is selected. If there is at least one minute of mixed precipitation and the most frequent type constitutes more than 70%, we assign the predominant type; otherwise, we classify the entire window as 'Mixed'.
- ROS Rain / Mixed / Snow: Every 6 min, the most frequently occurring type of precipitation inside the 3x3 km grid is selected. If there is at least one cell with mixed precipitation and the most frequent type constitutes more than 70%, we assign the predominant type; otherwise, we classify the entire grid as 'Mixed'.

Once the events are defined, two different contingency tables are generated to characterize the performance of each methodology. The first table is a 2x2 contingency table used to verify the performance of ROS in detecting precipitation against MRRs. The second table is a 3x3 multi-category contingency table, which evaluates ROS's ability to discriminate between different precipitation types.

Tables II and III present the contingency tables for MRR2, while Tables IV and V show the contingency tables for MRR-Pro. Various verification scores are computed, including Probability of Detection (POD), False Alarm Ratio (FAR), Critical Score Index (CSI), and Heidke Skill Score (HSS), as described by *Ghelli* (2009) (see Appendix).

B. Estimation of Rain or Snow In Height

The verification part of this study is constrained to surface level due to ROS being calculated using data from ground automatic stations. To evaluate the methodologies in the vertical dimension, height profiles need to be estimated. For this purpose, a Digital Elevation Model (DEM) with a resolution of 1 km has been used, providing estimated heights for each pixel within Catalonia. Utilizing a 21x21 km grid containing Das, which extends 14 km north, 7 km south, and 21 km east to west, the DEM was combined with ROS data, resulting in multiple arrays assigning heights and precipitation types. This particular grid was chosen to encompass the surrounding mountains, thereby achieving a greater vertical extension to mimic MRRs. However, the results from this estimation will not be verified, as the precipitation types obtained with ROS can come from points very distant from the observation one, and the heights obtained are not uniformly spaced. Instead, qualitative plots will be generated to illustrate what ROS would detect if extrapolated vertically.

This integration is useful for comparing the performance of ROS against ground-based observations, such as MRRs, especially in regions where terrain-induced radar beam blockage can significantly impact results.

Table II. Contingency table for precipitation events of MRR2 (observation) and ROS (forecast).

	MRR2 Observed	
ROS Forecast	**Precipitation**	**No precipitation**
Precipitation	788	1120
No precipitation	210	26545

Table III. Contingency table for multi-category events (Rain, Mixed or Snow) of MRR2 (observation) and ROS (forecast).

	MRR2 Observed		
ROS Forecast	**Rain**	**Mixed**	**Snow**
Rain	628	29	4
Mixed	16	6	12
Snow	14	23	56

Table IV. Contingency table for precipitation events of MRR-Pro (observation) and ROS (forecast).

	MRR-Pro Observed	
ROS Forecast	**Precipitation**	**No precipitation**
Precipitation	1162	746
No precipitation	1134	25621

Table V. Contingency table for multi-category events (Rain, Mixed or Snow) of MRR-Pro (observation) and ROS (forecast).

	MRR-Pro Observed		
ROS Forecast	**Rain**	**Mixed**	**Snow**
Rain	537	300	53
Mixed	6	10	31
Snow	17	61	147

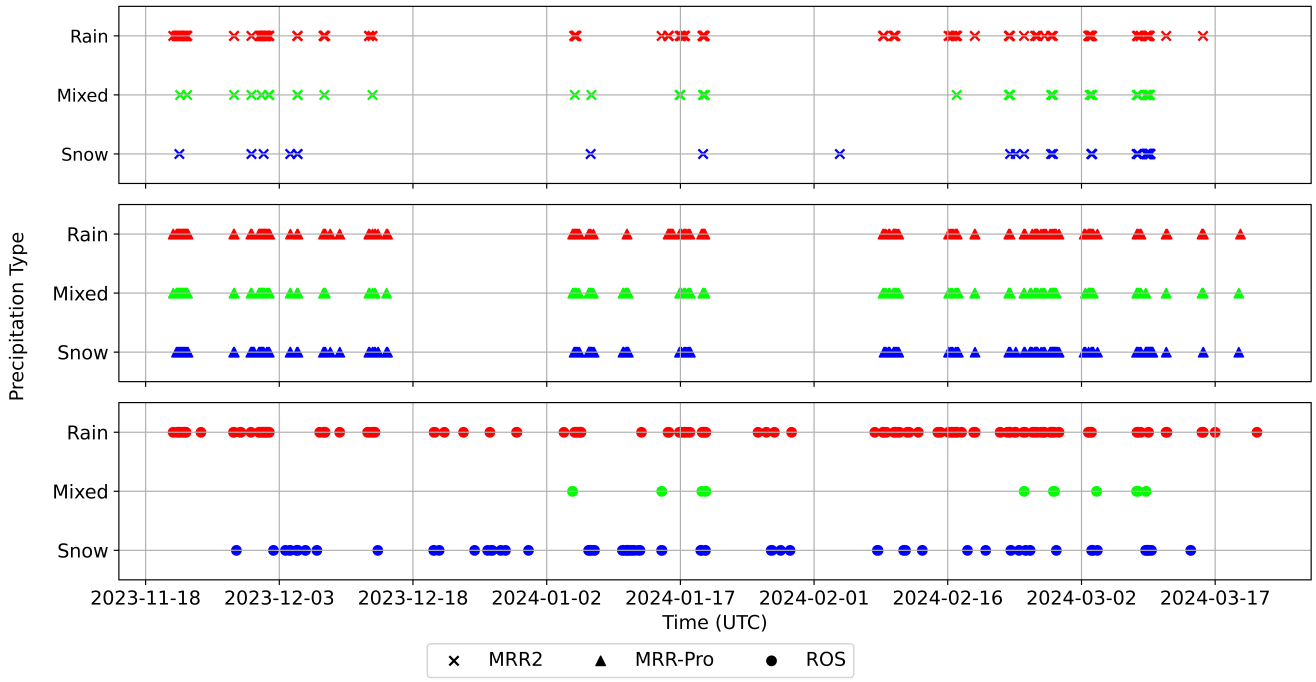

Figure 3. Precipitation type distribution for the study period, for each instrument (MRR2, MRR-Pro) after quality control and the closest pixel of ROS at surface level.

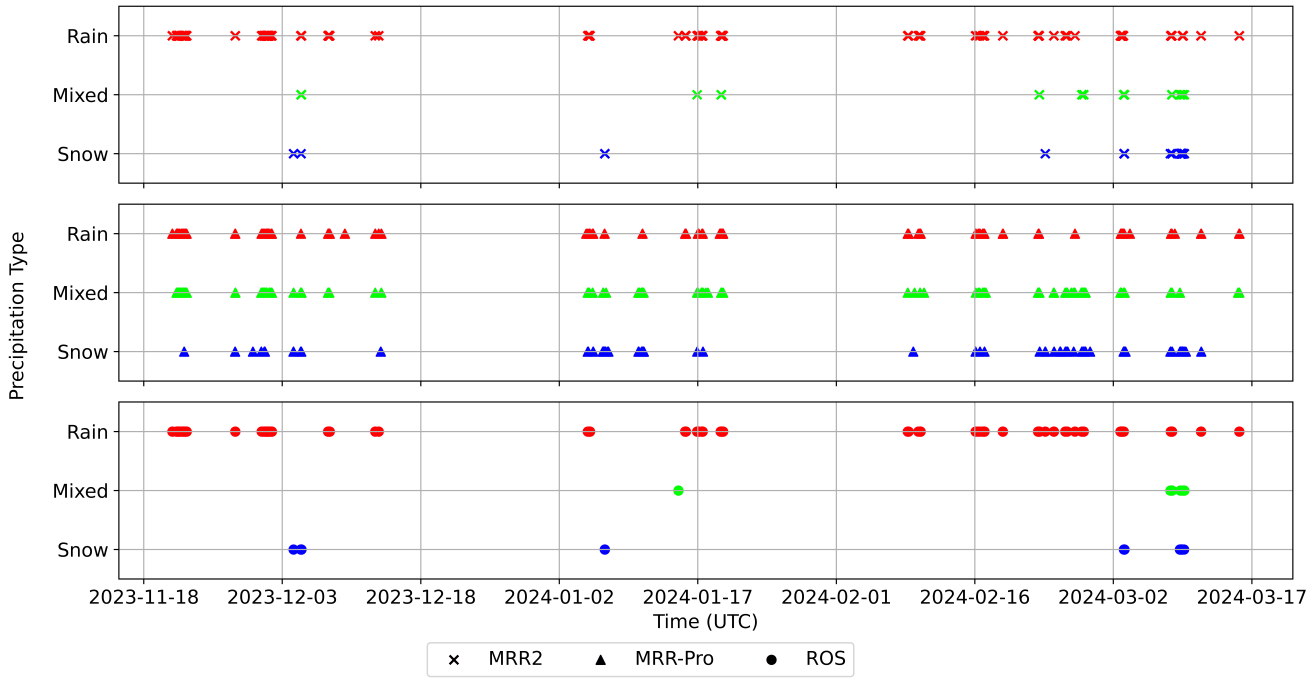

Figure 4. Precipitation type distribution for each instrument (MRR2, MRR-Pro) and ROS when considering only positive events of precipitation after applying fuzzy conditions.

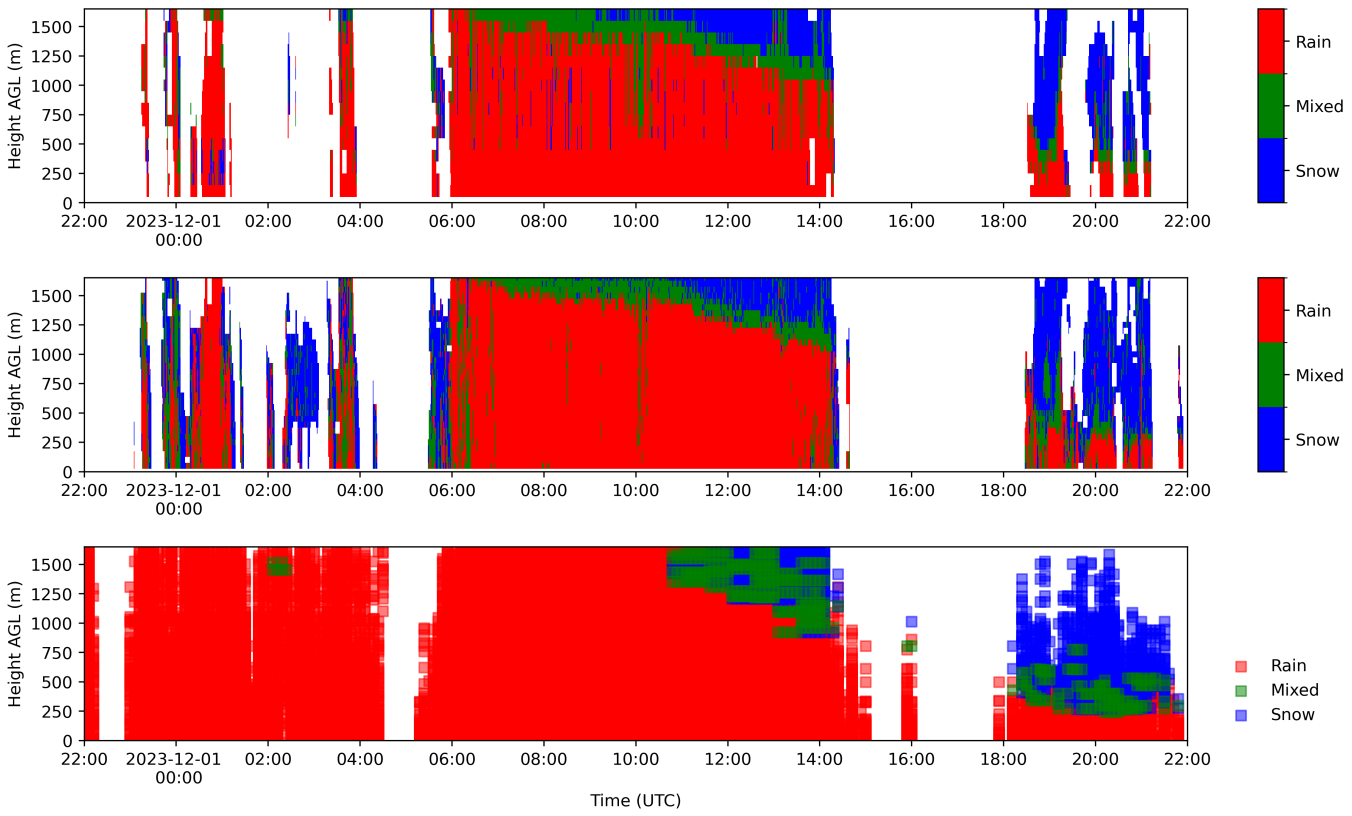

Figure 5. Time vs. height evolution of precipitation types corresponding to December 1st 2023 for all three methodologies of detection: MRR2 (top), MRR-Pro (middle), and ROS (bottom).

IV. RESULTS AND DISCUSSION

The results are presented in two distinct sections to align with the division of our methodology. Section A addresses the surface verification aspect, while Section B focuses on the qualitative analysis of the estimation of ROS at upper levels.

A. Surface Verification

To analyze the distribution of precipitation events, Figure 3 presents the occurrence of each precipitation type (rain, mixed, and snow) over time for the three methods: MRR2 (top), MRR-Pro (middle), and ROS (bottom), with ROS data values corresponding to the closest pixel to Das at surface level. The study period covers late autumn and winter months, including 15 episodes for both MRRs and 20 episodes for ROS, where an episode is defined as a period with more than one hour of continuous precipitation.

One notable characteristic is the absence of fully snowy days. Instead, there are only transitional episodes with changes between precipitation types. Another relevant point is that in December and late January, both MRRs recorded no precipitation, while ROS inferred up to five more episodes.

Table VI displays the verification metrics once events under fuzzy conditions have been defined. When comparing ROS with MRR2, a relatively high Probability of Detection (POD) is found, although the False Alarm Ratio (FAR) is also relatively large (greater than 0.5), resulting in a lower Critical Success Index (CSI) value. It is important to interpret these values considering how events are defined under fuzzy verification.

Table VI. Verification metrics comparing ROS against MRR2 and MRR-Pro at surface level. POD, FAR and CSI are calculated for precipitation detection (Tables II and IV), while HSS only for precipitation classification (Tables III and V).

Instrument	Precip. Detection	Precip. Classification
MRR2	POD = 0.790 FAR = 0.587 CSI = 0.372	HSS = 0.565
MRR-Pro	POD = 0.506 FAR = 0.391 CSI = 0.382	HSS = 0.305

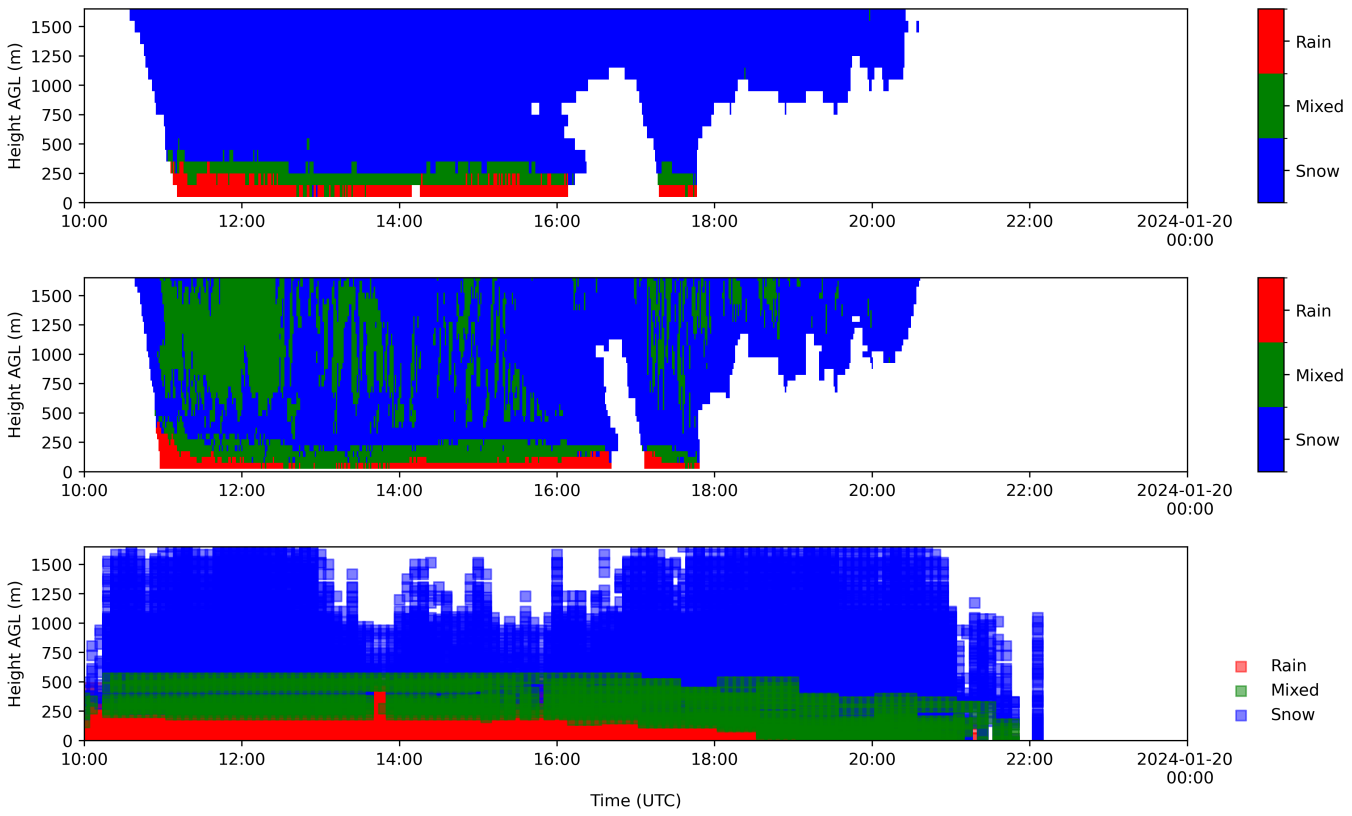

Figure 6. Time vs. height evolution of precipitation types corresponding to January 19th 2024 for all three methodologies of detection: MRR2 (top), MRR-Pro (middle), and ROS (bottom).

Because fuzzy verification has less restrictive temporal and spatial conditions, it results in higher POD values compared to point-to-point verification. However, this increase in POD is also accompanied by a higher FAR. Nonetheless, these results cannot be only attributed to fuzzy verification. As illustrated in Figure 3, the increased FAR could also be linked to the data gaps in December and January. While ROS diagnoses these as actual precipitation events, the MRRs do not detect them. A possible explanation could be due to their light and scattered nature, possibly not reaching the surface at Das.

Examining ROS against MRR-Pro, Figure 3 initially suggests a high POD for ROS, as it infers precipitation when MRR-Pro also observes precipitation. However, Table IV indicates that ROS has almost as many missed cases as hits, resulting in a relatively low POD. This low POD is partly mitigated by a moderately low FAR, leading to a CSI of 0.382, similar to the MRR2 case. Unlike with MRR2, the low POD can be attributed to MRR-Pro's more advanced technology and resolution, which captures finer and more detailed precipitation that ROS may not be able to diagnose. The FAR might be partially influenced by the gaps mentioned before, but it is not as high as when compared with MRR2.

Moreover, the verification of precipitation types reveals interesting patterns. Figure 4 displays positive events of precipitation, showing cases where both observation and forecast identify precipitation under the defined fuzzy conditions. Throughout the study period, MRR2 and ROS primarily identify rain, some snow, and occasional mixed precipitation; while MRR-Pro detects all three types with a denser data distribution. In December and late January, MRR2 and MRR-Pro exhibit data gaps, and ROS, which diagnosed some events during these periods in Figure 3, has these filtered when considering the events under fuzzy conditions.

ROS has the fewest cases of mixed precipitation, likely due to its narrow temperature threshold. Additionally, the definition of mixed precipitation events for MRRs in a temporal window tends to favor the mixed class, whereas ROS only considers spatial conditions inside the grid for each time step.

By computing the Heidke Skill Score (HSS), we are able to determine how capable is ROS at discriminating precipitation types. When compared with MRR2, ROS is quite a useful methodology for discriminating at surface level, with a HSS slightly greater than 0.5. Despite ROS's limitations in discriminating mixed precipitation, it effectively distinguishes between rain and snow. However, in comparison with MRR-Pro, ROS exhibits a HSS of 0.305, indicating a higher disagreement than with MRR2.

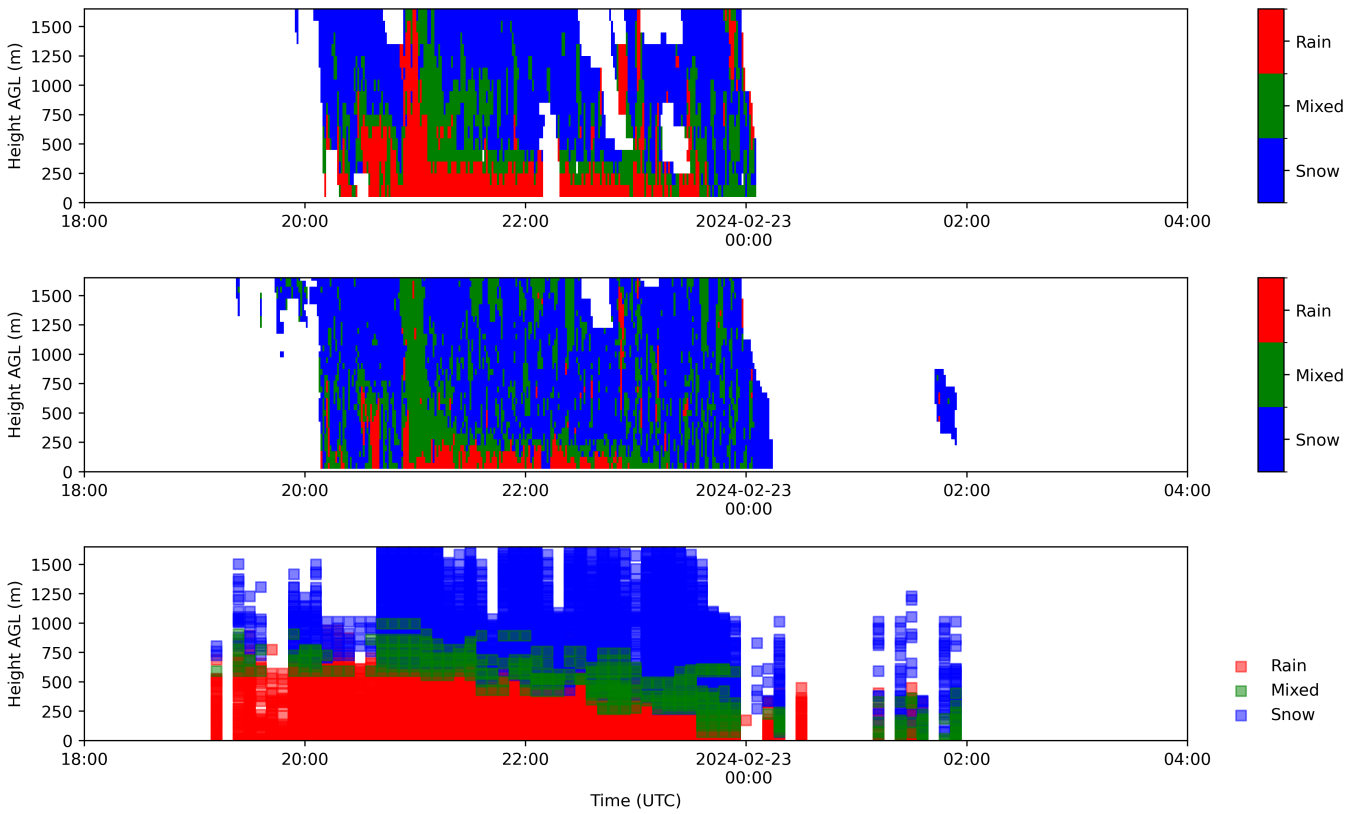

Figure 7. Time vs. height evolution of precipitation types corresponding to February 22nd 2024 for all three methodologies of detection: MRR2 (top), MRR-Pro (middle), and ROS (bottom).

B. In Height Qualitative Evaluation

For this section, three main episodes have been selected due to their interesting nature and display of all precipitation types considered. Figures 5, 6, and 7 show the temporal evolution of precipitation types for each methodology in height above ground level. Both MRRs display the integrated data after quality control, while for ROS, each data point (plotted as squares) represents a couple (height, type) as defined in Section III.B. The height range is limited to the maximum elevation that the DEM has inside the selected grid.

A preliminary overview indicates that, despite differences and considering the limitations of the estimation, ROS provides heights for each precipitation phase that are compatible with the observations made by the MRRs. Next, each episode will be analyzed separately.

1. December 1st 2023 episode

The episode shown in Figure 5 unfolds in three distinct phases: a short-lived precipitation at the start of the day, followed by a more sustained period lasting from 6 to 14 UTC and some transient precipitation at the end of the day, with the most interesting part occurring around midday.

Initially, ROS indicates a higher snow level compared to the MRRs. This discrepancy could arise from the differing approaches: MRR measures snow levels vertically in the free atmosphere, while ROS assesses the snow level at surface level. However, from 10 UTC onwards, ROS accurately reflects a descent in the snow level, that is also observed by the MRRs. Interestingly, this change in ROS from rain to mixed coincides with a downward trend in mixed precipitation detected by the MRRs.

Throughout the transient precipitation at the end of the day, all three methodologies consistently reflect a similar vertical hydrometeor distribution pattern and relatively close snow levels.

2. January 19th 2024 episode

During the January episode shown in Figure 6, the snow level remains consistently low, as diagnosed across all methodologies. However, ROS displays a slightly higher snow level and infers a significant 250 m thick layer of mixed precipitation, which is not as prominently displayed by the MRRs. This discrepancy occurs because ROS identifies mixed precipitation based on tempera-

ture thresholds and, throughout this event, precipitation types changed quickly. Moreover, the uneven spacing of ROS height data points, as discussed in section III.B., might also contribute to this difference.

Furthermore, ROS reports mixed precipitation at surface level towards the end of the episode, whereas the MRRs do not. This difference may be attributed to the fact that ROS data represent an entire 21 x 21 km grid, indicating that some locations within the grid could be experiencing precipitation not present in the vertical column above the MRRs.

MRR-Pro shows irregular patterns of mixed precipitation at various heights. This anomalous pattern is also observed in other episodes (not discussed here) and may be partially explained by the definition of thresholds within the classification algorithm, given that MRR-Pro is a more advanced model and that rapidly changing types have also been detected in the surface verification section.

This episode is particularly interesting because both MRRs detect an almost identical gap (probably corresponding to snow being lifted by the wind) between 16 and 18 UTC, a gap that ROS also identifies but at higher heights and during previous hours. Additionally, the MRRs exhibit consistent patterns at the beginning and end of the episode, effectively capturing the non-linear evolution of precipitation at different heights.

3. February 22nd 2024 episode

The last case presented was selected for its transition from rain to snow at surface level. During the February episode, shown in Figure 7, the snow level fluctuates abruptly at various points. This variability is clearly shown in the MRR-Pro plot, which displays all three types of precipitation at different levels in a chaotic manner, indicating significant mixing conditions.

Similar to the previous case, ROS demonstrates a higher snow level but shows less variability than the MRRs. Nonetheless, ROS accurately captures the trend of the descending snow level observed by the MRRs.

By the end of the episode, both MRR2 and ROS show mixed precipitation at surface level, while MRR-Pro detects snow, once again highlighting the very high variability of this episode.

V. CONCLUSIONS

This study examines episodes of transitions between precipitation types at both surface and upper levels in La Cerdanya valley. Using a fuzzy verification approach, the following results were obtained when comparing an operational product with instrumental observations.

For surface-level detection of precipitation events, the metrics indicated that, when compared with MRR2, ROS exhibited a high POD but also a high FAR, resulting in a lower CSI. The high FAR could be attributed to the data gaps observed during December and late January, periods during which both MRR2 and MRR-Pro observed no precipitation, whereas ROS inferred five additional episodes. This discrepancy may be due to light and scattered precipitation above the valley, which only ROS's radar data is capable of detecting.

Although ROS did not exhibit such a high FAR when compared with MRR-Pro, it had nearly as many missed events as hits, leading to a relatively low POD. This could be due to MRR-Pro's advanced technology capturing finer transitional details that ROS is not capable of detecting.

Regarding surface-type classification, MRR2 and ROS consistently identified rain and sporadically mixed and snow precipitation, while MRR-Pro detected all three types with a denser data distribution. In terms of mixed precipitation, ROS had the fewest cases, likely due to its narrow temperature threshold, whereas MRR methodologies favored the mixed class because of the defined fuzzy temporal conditions.

When evaluating performance through HSS, ROS is quite a useful methodology for discriminating at surface level when compared to MRR2. However, in comparison with MRR-Pro, ROS exhibits a lower level of agreement.

As for the upper level qualitative evaluation, ROS showed compatibility with the heights observed by MRRs for each precipitation type, despite methodological differences. For instance, ROS tended to indicate a higher snow level during the January and February episodes but accurately captured trends observed by the MRRs. Similarly, in the January episode, ROS detected a wider layer of mixed precipitation not observed by the MRRs, likely due to both the temperature threshold and heights considered by ROS.

Overall, ROS and MRR2 exhibited comparable performance in discriminating precipitation types at surface level within the valley. In contrast, the more advanced technology of MRR-Pro, proved to be incompatible with ROS for this specific task. Lastly, ROS height estimates showed compatibility with the MRRs observations.

Future work could explore the uncertainty associated with the verification metrics and develop a nowcasting product to forecast precipitation types at very short temporal ranges.

VI. APPENDIX

This appendix provides additional information to aid in the correct interpretation of the verification metrics. Table VII presents the standard format of a 2x2 contingency table.

The ideal scores are as follows: POD, CSI, and HSS equal to 1, while FAR equal to 0.

Definitions of the verification scores used are given by:

Table VII. Standard definition of a 2x2 contingency table.

	Event Observed	
Event Forecast	**Yes**	**No**
Yes	Hits	False Alarms
No	Misses	Correct Negatives

$$\text{POD} = \frac{\text{hits}}{\text{hits} + \text{misses}}$$

$$\text{FAR} = \frac{\text{false alarms}}{\text{hits} + \text{false alarms}}$$

$$\text{CSI} = \frac{\text{hits}}{\text{hits} + \text{false alarms} + \text{misses}}$$

$$\text{HSS} = \frac{N \cdot (\text{hits} + \text{correct negatives}) - (\text{misses} + \text{false alarms}) \cdot (\text{false alarms} + \text{misses})}{(N + \text{hits} + \text{false alarms}) \cdot (\text{misses} + \text{false alarms} + \text{correct negatives})}$$

where N = hits + misses + false alarms + correct negatives.

ACKNOWLEDGMENTS

Without the support of many people, this master's thesis could not have been completed. I want to start by thanking Joan Bech, my advisor, for his expertise and comments. In addition, I would like to express my gratitude to everyone at SMC who offered their generous help, especially J.R. Miró and Enric Casellas. Finally, I would also like to thank my family and friends for their continuous encouragement throughout every stage of my career.

REFERENCES

Bech, J., B. Codina, J. Lorente, and D. Bebbington, The Sensitivity of Single Polarization Weather Radar Beam Blockage Correction to Variability in the Vertical Refractivity Gradient, *Journal of Atmospheric and Oceanic Technology*, *20*(6), 845 – 855, doi:10.1175/1520-0426(2003)020¡0845:TSOSPW¿2.0.CO;2, 2003.

Casellas, E., J. Bech, R. Veciana, N. Pineda, T. Rigo, J. R. Miró, and A. Sairouni, Surface precipitation phase discrimination in complex terrain, *Journal of Hydrology*, *592*, 125,780, doi: https://doi.org/10.1016/j.jhydrol.2020.125780, 2021.

Conangla, L., J. Cuxart, M. A. Jiménez, D. Martínez-Villagrasa, J. R. Miró, D. Tabarelli, and D. Zardi, Cold-air pool evolution in a wide Pyrenean valley, *International Journal of Climatology*, *38*(6), 2852–2865, doi: https://doi.org/10.1002/joc.5467, 2018.

Ebert, E. E., Fuzzy verification of high-resolution gridded forecasts: a review and proposed framework, *Meteorological Applications*, *15*(1), 51–64, doi:10.1002/met.25, 2008.

Garcia-Benadi, A., J. Bech, S. Gonzalez, M. Udina, B. Codina, and J.-F. Georgis, Precipitation Type Classification of Micro Rain Radar Data Using an Improved Doppler Spectral Processing Methodology, *Remote Sensing*, *12*(24), doi: 10.3390/rs12244113, 2020.

Garcia-Benadi, A., J. Bech, M. Udina, B. Campistron, and A. Paci, Multiple Characteristics of Precipitation Inferred from Wind Profiler Radar Doppler Spectra, *Remote Sensing*, *14*(19), doi:10.3390/rs14195023, 2022.

Ghelli, A., Verification of categorical predictands, `https://www.swpc.noaa.gov/sites/default/files/images/u30/Verification%20of%20Categorical%20Predictands.pdf`, [Accessed 30-06-2024], 2009.

González, S., J. Bech, A. Garcia-Benadí, M. Udina, B. Codina, L. Trapero, A. Paci, and J.-F. Georgis, Vertical structure and microphysical observations of winter precipitation in an inner valley during the Cerdanya-2017 field campaign, *Atmospheric Research*, *264*, 105,826, doi: https://doi.org/10.1016/j.atmosres.2021.105826, 2021.

Kochendorfer, J., R. Nitu, M. Wolff, E. Mekis, R. Rasmussen, B. Baker, M. E. Earle, A. Reverdin, et al., Analysis of single-Alter-shielded and unshielded measurements of mixed and solid precipitation from WMO-SPICE, *Hydrology and Earth System Sciences*, *21*(7), 3525–3542, doi: 10.5194/hess-21-3525-2017, 2017.

SMC, Atles climàtic 1991-2020. Meteocat, `https://www.meteo.cat/wpweb/climatologia/el-clima/atles-climatic/`, [Accessed 01-07-2024], 2024.

Xercavins, A., Els climes del Pirineu Oriental: des de les terres gironines fins a la Catalunya Nord i Andorra, *Documents d'Anàlisi Geogràfica*, (7), 81–102, 1985.